Cryst. Res. Technol. **39**, No. 11, 969 – 979 (2004) / **DOI** 10.1002/crat.200410282

Diffusion induced segregation in the case of the ternary system sphalerite, chalcopyrite and cubanite

T. Blesgen*[1], S. Luckhaus[2], and K. Bente[3]

[1] Max-Planck-Institute for Mathematics in the Sciences, Inselstraße 22-26, 04109 Leipzig, Germany
[2] Faculty for Mathematics and Computer Science, University of Leipzig, Augustusplatz 10-11, 04103 Leipzig, Germany
3 Institute for Mineralogy, Crystallography and Materials Science, University of Leipzig, Scharnhorststraße 20, 04275 Leipzig, Germany

Received 28 June 2004, accepted 1 July 2004
Published online 1 October 2004

Key words structure gradients, phase transitions, ternary systems.
PACS 61.43.BN, 64.75.+g, 81.10.Aj

A mathematical model for describing natural and experimental diffusion induced segregation (DIS) in the case of a (Zn,Fe)S single crystal with three coexisting phases is derived. As main result, a new and quite general segregation principle for ternary systems is discovered where one phase has a flat free energy density and serves as catalyst for the segregation of the other two phases. The model includes also a stochastic noise term to represent fluctuations of the copper concentration. Numerical simulations in 2-d underline the physical significance of the model and allow to make quantitative predictions.

1 Introduction

This article is the continuation of the work [1] where the so-called chalcopyrite disease within sphalerite was studied. Hereby the reaction models concerning atomistic mechanisms implying vacancy and metal diffusion as well as redox conditions from experimental DIS (Diffusion Induced Segregations) were used for the mathematical simulations. The corresponding experimental studies simulating natural DIS show that primary sphalerites bearing Fe > 3 at. % can be provoced to show DIS of Cu-Fe-S-phases, if firstly Fe^{2+} is oxidized to Fe^{3+} by increasing sulfur fugacity. If then Cu diffuses into these sphalerites Cu reacts with Fe^{3+} to form e.g. chalcopyrite(ccp), i.s.s. (intermediate solid solution within the Cu-Fe-S-system) or "cubanite" ($CuFe_2S_3$). The natural phenomena and experimental results for i.s.s.-respectively DIS-ccp are exemplary shown in Figures 1 to 4. The corresponding data verify the experimental results and interpretations to be in agreement to natural DIS reactions.

Starting from former mathematical simulations only concerning two phase reaction phenomena we are going to extend these results to a ternary system where beside the two phases sphalerite and chalcopyrite, cubanite is present as third phase. Subsequently it is transferred by Cu-enrichment in the main DIS-phases. This is important for the extension of experimental situations to natural conditions and to common material science phenomena and to understand very first DIS stages. The third phase is only occuring in submicroscopic dimensions and only in status nascendi. As main result of our analysis we will show that cubanite can be regarded as precursor to the formation of chalcopyrite. Significant improvements are incorporated into the mathematical formulation, in particular the phase transitions are now formulated as sharp interfaces and a stochastic term accounts for fluctuations of the copper concentration on the micro scale. An additional new

* Corresponding author: e-mail: blesgen@mis.mpg.de

aspect is that the phase parameter is now the *global* minimiser of the free energy; we will discuss that issue in length in Section 3.

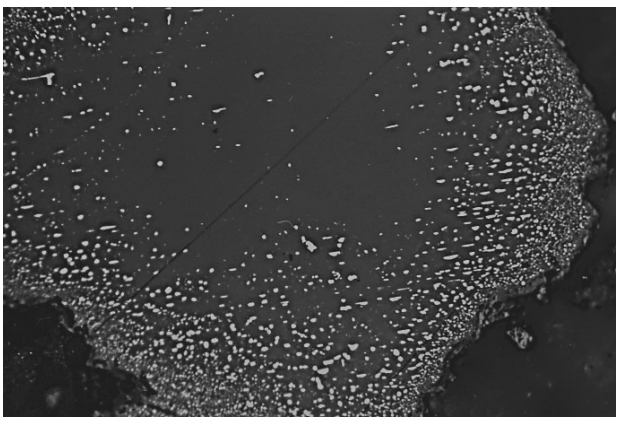

Fig. 1 Fe-bearing sphalerite crystal (grey) with DIS-ccp (light) from mineralized hydrothermal veins of East Banke, Nigeria. At the rim of the crystal the DIS-particles are fine-grained, whereas towards to the core the segregation particles become larger due to coarsening. Width of LM-micrograph 420µm, reflected light, 1. Polar., oil.

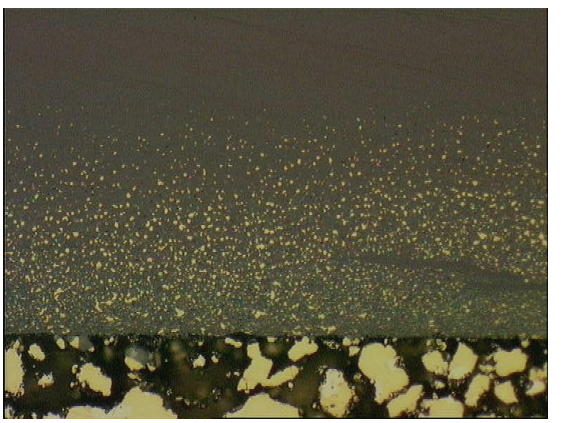

Fig. 2 Experimental simulation of DIS-i.s.s. using natural Fe-bearing and exsolution free sphalerite (grey) from St. Cristoph, Saxony. The crystal was embedded in synthetic Fe-rich i.s.s. (yellow, Fe/Cu=1.3) to run at T=573K over t=14d at a relatively high sulfur fugacity of the $CuS/Cu_{2-x}S$ buffer. The experiment yields a fine-grained DIS-bearing rim (yellow) in the primary sphalerite crystal. Width of LM-micrograph: 125µm, reflected light, Polar., oil.

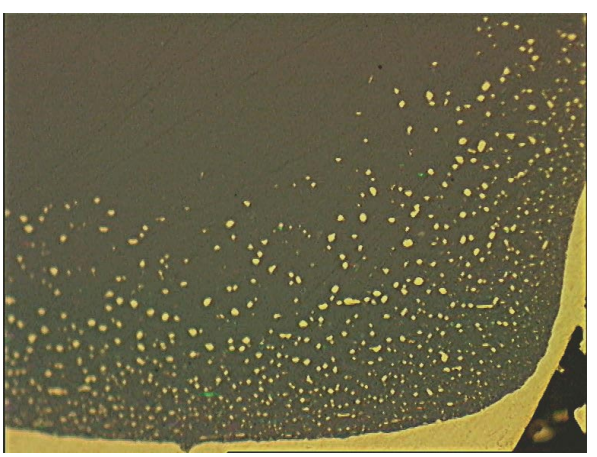

Fig. 3 Experimental simulation of DIS-i.s.s. (yellow) using a synthetic Fe-bearing sphalerite crystal (grey) embedded in a Fe-rich i.s.s. (yellow, Fe/Cu=1.3). Experimental parameters are T=873K for t=7d at the sulfur fugacity of the $Fe_{1-x}S/FeS_2$ buffer. The resulting microphenomena show that the former sphalerite rim is partially replaced by dense i.s.s. (yellow). A possible third phase as primary exsolution cannot be seen because of submicroscopic dimensions. Within the remaining sphalerite (grey) tiny DIS-particles (yellow) occur which are followed up by coarsened exsolution particles (yellow) towards the core of the crystal. Width of LM-micrograph: 125µm, reflected light, Polar., oil.

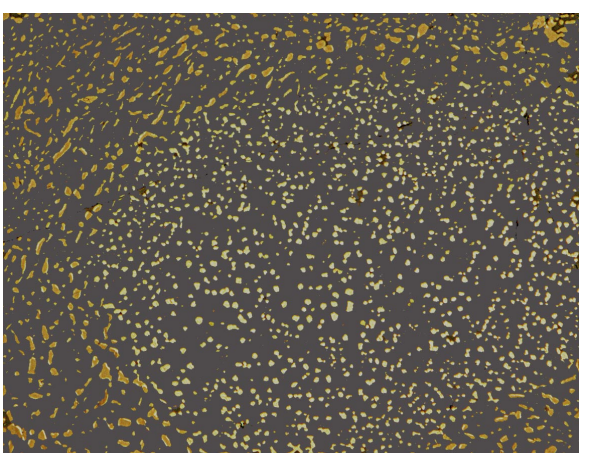

Fig. 4 Experimental simulation of DIS-i.s.s. (light) and DIS-bn (brownish) as a third phase using a synthetic Fe-bearing sphalerite crystal (grey) embedded in bornite (Cu_5FeS_4, bn). Experimental parameters are T=973K for t=2d at the sulfur fugacity of the $Fe_{0.920}S$ buffer. The resulting microphenomena show abundant DIS-i.s.s. in the core of the sphalerite surrounded by DIS-bn. I.s.s. is tranformed to bornite in the outer parts of the sphalerite crystal due to Cu-enrichment which also leads to coarsening of the DIS-grains. Width of LM-micrograph: 220µm, reflected light, Polar., oil.

The main result of our analysis is the understanding of how cubanite triggers the segregation of sphalerite and chalcopyrite. We will find that cubanite is important in the early stages of DIS to lower the activation energy and to start the segregation. In the late stages, it only occupies a small part of the crystal (which is maybe the reason why its role has been ignored up to now). With regard to these facts, the mechanism we find is named 'catalytic segregation principle' in this article. It is probable that similar phenomena can be observed in other materials and that the documented mechanism is not restricted to sulphide systems alone.

2 Derivation of the mathematical model

We introduce functions $c_i = c_i(x,t)$ that trace the concentrations of the involved constituents at time t and space point $x \in \Omega$ where Ω is a (time-independent) domain in R^D, $1 \le D \le 3$ that is occupied by the crystal. In particular we introduce $c_1 \approx Fe^{3+}$, $c_2 \approx Fe^{2+}$, $c_3 \approx Cu^{+}$, $c_4 \approx Zn^{2+}$, $c_5 \approx$ vacancies.

Reflecting the conditions during the crystallographic experiments we will assume that the temperature T is held constant. This also simplifies the formulation within the framework of non-equilibrium thermodynamics.

As explained in [1] we will assume the relationship $c_5 = \frac{1}{2} c_1$ that can be deduced from the electric neutrality of the crystal and which has been verified by the crystallographic measurements. Furthermore we introduce $c_6 \equiv \frac{1}{2}$, the (constant) concentration of sulphur. For a concentration vector $c = (c_1, \ldots, c_4)$ the free energy density of phase l is denoted by f_l, where throughout this article $l = 1$ stands for chalcopyrite, $l = 2$ for sphalerite and $l = 3$ for cubanite.

For $f_l(c)$ we make the order-disorder approach

$$f_l(c) = \sum_{i=1}^{4} \beta_i^l c_i \ln c_i + \left(\sum_{i=1}^{4} \alpha_i c_i \right)^2 . \tag{1}$$

The constants β_i^l and α_i are positive. The second term in (1) measures the volume response when replacing Zn^{2+} by other metal ions. The ansatz (1) is reasonable because the high temperature transitions are random pairwise interactions.

We introduce three functions $\chi_l = \chi_l(x,t) \in \{0,1\}$, $1 \le l \le 3$ that measure the volume fraction of phase l. These indicators fulfil $\chi_1 + \chi_2 + \chi_3 \equiv 1$, thus with known vector of phase functions $\chi = (\chi_1, \chi_2)$, the volume fraction $\chi_3 := 1 - \chi_1 - \chi_2$ of cubanite is also known. Technically speaking χ_l are functions of bounded variation, see [9]. Since 0 and 1 are the only possible values of χ_l, every point $x \in \Omega$ corresponds to exactly one of the three phases. Thus, unlike the former model for chalcopyrite disease, no 'mushy regions' occur during the computations and the interfaces at the phase boundaries are sharp.

Since the bulk free energy density is the convex hull of $\{f_1, f_2, f_3\}$, as a consequence of the thermodynamic identity $F = E - TS$, we write the total free energy of the system in the form

$$F(c,\chi) = \int_\Omega f(c,\chi) = \int_\Omega \sum_{l=1}^{3} \chi_l f_l(c) + T \int_\Omega s_M(\chi)$$

with the mixing entropy density

$$s_M(\chi) = W(\chi) + \varepsilon(|\nabla \chi_1| + |\nabla \chi_2|)$$

and the double well potential

$$W(\chi) := \sum_{l=1}^{3} \chi_l \quad \ln \chi_l.$$

The term ε in the definition of s_M is related to the surface tension of the transition layer between two neighbouring interfaces and $\int_\Omega |\nabla \chi_l|$ is the total variation of χ_l in Ω.

The constitutive relation for the mass fluxes J_i is assumed to be of the isotropic Onsager form

$$J_i = \sum_{j=1}^{4} L_{ij} \nabla \mu_j,$$

where the mobility L is a symmetric positive-semidefinite 4x4 tensor and $\mu = (\mu_1, \ldots, \mu_4)$ denotes the vector of chemical potentials with

$$\mu_j = \frac{\partial F}{\partial c_j}.$$

For the control mechanism of the vector $\chi = (\chi_1, \chi_2)$ of phase parameters we introduce the equation

$$(\chi_1, \chi_2) = \arg\min_{(\tilde{\chi}_1, \tilde{\chi}_2)} \quad F(c, \tilde{\chi}_1, \tilde{\chi}_2), \tag{3}$$

where $(\tilde{\chi}_1, \tilde{\chi}_2)$ fulfil the constraints on χ_l presented above. Equation (3) states that χ_l are *global* minimisers - a fact that is crucial for our analysis. In this regard the model differs significantly from the model for chalcopyrite disease within sphalerite. The ideas behind this ansatz are explained in Section 3.

Now we can state the complete model:

Find for $t \geq 0$ functions $c_1,\ c_2,\ c_3,\ c_4, \chi_1, \chi_2$ such that in $\Omega \subset \mathrm{R}^D$ for $t > 0$

$$\partial_t c_i = \operatorname{div}\left(\sum_{j=1}^{4} L_{ij} \nabla \tfrac{\partial f}{\partial c_j}(c, \chi) \right),\ 1 \leq i \leq 4, \tag{2}$$

$$(\chi_1, \chi_2) = \arg\min_{(\tilde{\chi}_1, \tilde{\chi}_2)} \quad F(c, \tilde{\chi}_1, \tilde{\chi}_2), \tag{3}$$

$$c_i(x, 0) = c_{0i}(x),\ 1 \leq i \leq 4, \tag{4}$$

$$\chi_l(x, 0) = \chi_{0l}(x), \quad l = 1, 2 \tag{5}$$

$$\partial_\nu c_1 = \partial_\nu c_2 = \partial_\nu c_4 = \partial_\nu \chi_1 = \partial_\nu \chi_2 = 0,\ c_3 = g_3 \tag{6}$$

with initial conditions for $t = 0,\ x \in \Omega$ and boundary conditions for $t > 0,\ x \in \partial\Omega$.

Neumann boundary conditions (6) are essential to affirm mass conservation for c_1, c_2, c_4 which is $\int_\Omega c_i(x,t)\ dx = \int_\Omega c_{0i}(x)\ dx$ for $i = 1, 2, 4$ and every $t > 0$. This leads to a coupling of the concentration components which is a decisive property for the validity of the segregation principle as we shall see.

3 A catalytic segregation principle

In order to explain this segregation principle, we first restrict to special cases and keep the argumentation simple. Later we will treat the general case.

Eq. (3) states that $\chi = (\chi_1, \chi_2)$ is a global minimiser of F. We assume for the moment that the concentration vector has only one component, i.e. $c = c_1$. By $\overline{c}_l$ we denote the concentration value where $f_l(c)$ attains its minimum. We introduce 4 constants $c_{13}^{\pm}$, $c_{23}^{\pm}$ which are uniquely specified by the conditions

$$f_1(c_{13}^{\pm}) = f_3(c_{13}^{\pm}), \qquad c_{13}^{-} < \overline{c}_1 < c_{13}^{+} < \overline{c}_3, \tag{7}$$

$$f_2(c_{23}^{\pm}) = f_3(c_{23}^{\pm}), \qquad c_{23}^{-} < \overline{c}_3 < c_{23}^{+} < \overline{c}_2. \tag{8}$$

The constants $c_{13}^{\pm}$, $c_{23}^{\pm}$ allow to determine directly for every concentration c which of the three phases has smallest bulk free energy density.

Let at $t = 0$ only sphalerite and cubanite be present occupying volumes V_2 and V_3. Additionally we neglect the surface energy and assume that c is constant in each of the sets V_2 and V_3, thus $c_0 \equiv B$ in V_2 and $c_0 \equiv C$ in V_3 for suitable constants B and C. To fix the initial conditions we want to assume that

$$c_{13}^{+} < C < \overline{c}_3, \qquad c_{23}^{-} < B < \overline{c}_2. \tag{9}$$

Now we will investigate the time evolution of c starting from this initial data. Let at time $t_1 > 0$ sphalerite occupy a volume $\tilde{V}_2$, cubanite a volume $\tilde{V}_3$ and let $c \equiv \tilde{B}$ in $\tilde{V}_2$, $c \equiv \tilde{C}$ in $\tilde{V}_3$. Throughout the text ˜ refers to data at time t_1.

As a consequence of the minimisation rule (3), for every point in Ω the smallest bulk free energy determines the dominant phase and consequently

$$\tilde{V}_l = \left\{ x \in \Omega \mid f_l(\tilde{c}(x)) = \min_{j=1,2,3} f_j(\tilde{c}(x)) \right\}. \tag{10}$$

Assuming that the change $\tilde{C} - C$ is not too large such that still $c_{13}^{+} < \tilde{C} < c_{23}^{-}$, we find with (10) that $\tilde{V}_2 = V_2$ and $\tilde{V}_3 = V_3$.

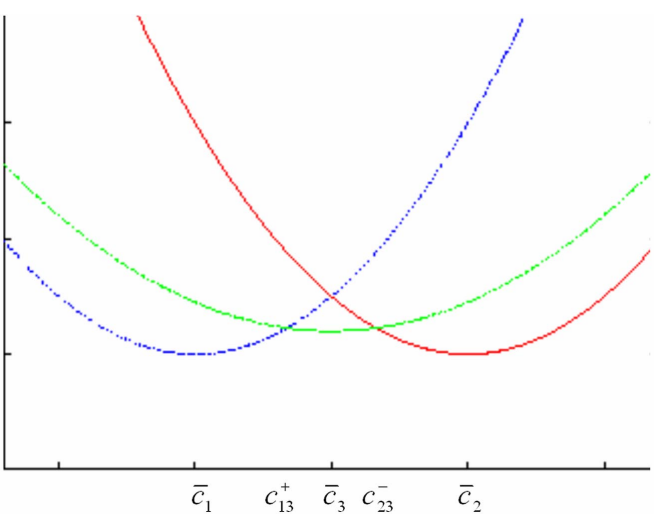

Fig. 5 Sketch of the free energy densities of the ternary system if c has only one component.

By mass conservation, the concentrations $\tilde{B}$ and $\tilde{C}$ are coupled by the relation

$$|V_2| \, (\tilde{B} - B) = |V_3| \, (C - \tilde{C}).$$

This allows to write $\tilde{C}$ as a function of $\tilde{B}$:

$$\tilde{C}(\tilde{B}) = \frac{\overline{c} - \tilde{B}\,|V_2|}{|V_3|}. \tag{11}$$

Here, $\overline{c} = \int_\Omega c_0$ is the average of c over Ω which due to mass conservation is invariant with respect to time.

With (11) we find that the free energy at time t_1 for the two phase configuration is

$$F(\tilde{B}) = |V_2|\, f_2(\tilde{B}) + |V_3|\, f_3(\tilde{C}(\tilde{B}))$$

and this yields at once

$$\frac{\partial F}{\partial \tilde{B}}(\tilde{B}) = |V_2|\left[f_2'(\tilde{B}) - f_3'(\tilde{C}(\tilde{B})) \right] .$$

For the setting fixed by (9) we infer that $\frac{\partial F}{\partial \tilde{B}}(\tilde{B}) < 0.$ This indicates that the free energy can be lowered by an increase of $\tilde{B}$ which by Formula (11) goes along with a decrease of $\tilde{C}$. The dynamic behaviour of c starting from initial data (9) is now clear: During the evolution, $\tilde{C}$ decreases more and more, until at some moment $\tilde{C} < c_{13}^{+}$ which means that for this concentration, the chalcopyrite phase has the lowest energy value and the cubanite phase flips over to chalcopyrite. Hence we end with a distribution of sphalerite and chalcopyrite where we started with sphalerite and cubanite. This puts some light on the principle we want to study.

At this point, some comments are in place about the nature of the phenomenon and the assumptions made during the above exemplary derivation.

1. The energy barrier between chalcopyrite and sphalerite (for the binary system) is significantly higher than the barriers between chalcopyrite and cubanite and between cubanite and sphalerite (for the ternary system), as Figure 5 illustrates. Therefore the segregation of the ternary system sphalerite-cubanite-chalcopyrite starts at much smaller spatial variations of c than this is the case for the binary system sphalerite-chalcopyrite. Thus we see that cubanite helps in the segregation of the other two phases. In the later stages of the dynamic process we found above that cubanite disappears in most of the domain. Therefore it makes sense to speak of a *catalytic segregation principle* where cubanite is the catalyst for the segregation of sphalerite and chalcopyrite.
2. The flatness of f_3 in comparison to f_1 and f_2 is essential for the functioning of the principle. Not only that this lowers the energy barriers, furthermore as a rule of thumb we can say that the flatter f_l, the faster the change in time of c in V_l. Therefore, the concentration in cubanite is the first to pass one of the thresholds c_{13}^{+} or c_{23}^{-} leading to the disappearance of this phase. From (11) we can read off how the rule of thumb is weakened if the volume V_3 of the third phase at $t = 0$ is considerably larger than V_2.
3. Mass conservation is also essential for the functioning of the principle as it couples the concentrations of c in V_l. In the above discussion we deduced from (11) that an increase of $\tilde{B}$ implies a decrease of $\tilde{C}$. This is no longer true if the mass of c may vary.
4. The simplifying assumptions we made above are no severe restrictions: (a) The constancy of c within a single phase is asymptotically true for large times t (because diffusion is smearing out the spatial differences of c). The same argument also explains why we could disregard the surface energy (because

the surface energy is important only for a small region close to the transition layers and not for the bulk region). (b) The constancy assumption on c neglects one important aspect: If c is continuous (e.g. growing from $\overline{c}_1$ to $\overline{c}_2$), there remains a small layer between sphalerite and chalcopyrite with $c \approx \overline{c}_3$ in which cubanite has smallest free energy density. This small layer does not disappear. (c) The choice (9) on the initial conditions was only made to select one scenario. Other two-phase settings lead to analogous results: The concentration $\tilde{B}$ in sphalerite approaches the minimal value $\overline{c}_2$ and the concentration in cubanite changes opposite to it in order to ensure conservation of mass. (d) If c has more than one component, the above argumentation can be repeated independently for each entry provided mass conservation holds for this co-ordinate. Thus the presented dynamic holds for c_1, c_2 and c_4. The concentration c_3 of Cu^+ is different, more on this in Section 3. (e) If all three phases are simultaneously present and if the occupied volumes are the same, the phase j with steepest free energy density will dominate the others and the concentration with respect to this phase will move towards the minimum $\overline{c}_j$. The other phases will follow this shift according to mass conservation. If the occupied volumes are different, this effect is weakened like in the case of two coexisting phases.

5. We want to explain the difference between Equation (3) and the Allen-Cahn ansatz used in the model of chalcopyrite disease within sphalerite. The Allen-Cahn model must be vector-valued to fit to the ternary system. The correct formulation is for $l = 1, 2$ where $\psi_l = \partial F / \partial \chi_l$ is the derivative of the potential F where F looks as in Figure 6 with three disjoint minima.

$$\partial_t \chi_l = \varepsilon^2 \Delta \chi_l - \psi_l(c, \chi_1, \chi_2), \tag{12}$$

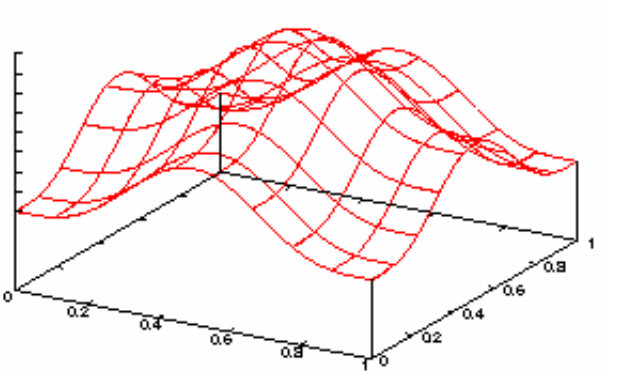

Fig. 6 Potential F with the three minima at (0,0), (1,0) and (0,1).

Figure 6 shows the potential F for a fixed value of c plotted as a function of χ_1 and χ_2. Admissible values of (χ_1, χ_2) are contained within the triangle with corners (1,0) (chalcopyrite), (0,1) (sphalerite) and (0,0) (cubanite) even though Figure 6 displays the entire square. These three corners are at the same time the positions of the local minima of F. The evolution of (χ_1, χ_2) governed by (12) starts for every $x \in \Omega$ randomly with a χ close to the maximum $\chi_1 = \chi_2 = 0.5$ and moves (inside the triangle of admissible χ) downhill to one of the three minima. The location of the reached minimum determines the phase in x. Once a local minimum has been reached, (χ_1, χ_2) becomes stationary and does not change any more. This demonstrates why the Allen-Cahn ansatz is not suitable to model the investigated ternary system. Using (12), the phase parameter will stay in a local minimum, for instance cubanite, even if another phase, i.e. chalcopyrite, has a smaller free energy value. Thus, no flipping over from cubanite to chalcopyrite is possible for a model that relies on Equation (12).

In continuation of the last argument, we will now explain the role of c_3 and take the effect of diffusion induced segregation into account. If a sufficient amount of copper has penetrated the matrix, chalcopyrite becomes energetically favourable whereas for small values of c_3, sphalerite has the smallest free energy. Looking at Figure 6 this means that the local minimum at (1,0) (chalcopyrite) is to be decreased for larger c_3 whereas the local minimum at (0,1) (sphalerite) has to be increased (the phase parameter controlled by the global minimisation (3) does not move along a path as in the Allen-Cahn evolution but jumps directly to the global minimum). In this way DIS is also taken into account in the binary model of chalcopyrite disease within sphalerite. Energy minimisation automatically leads to a preference of chalcopyrite in copper rich regions.

As the experimental results of both the binary and the ternary system clearly demonstrate, chalcopyrite forms complicated patterns in the vicinity of the crystal boundary. This is the result of different nucleation speeds in different parts of the single crystal and a competition of surface energy and volume energy. It is our firm belief that impurities play a crucial role as nucleation centres in the early stages of segregation, but more mineralogical experiments must be carried out in this direction to understand this complex matter.

Up to that point, the model we developed represents a perfect homogeneous material without impurities. The chalcopyrite interface predicted by that model would be perfectly regular following the copper front moving inward towards the crystal centre. In order to account for different segregation speeds, we lower/increase the minima of the potential F by stochastic fluctuations. A stochastic source term in the context of spinodal decomposition has first been introduced by Cook [5]. Langer [7] has also developed a statistical theory of spinodal decomposition leading to a Fokker-Planck equation.

In our case this means

$$f_1(c) = \beta_1 \sum_i \; c_i \ln c_i + \left(\sum_{i=1}^{4} \alpha_i c_i \right)^2 + m(c_3),$$

$$f_2(c) = \beta_2 \sum_i \; c_i \ln c_i + \left(\sum_{i=1}^{4} \alpha_i c_i \right)^2 - m(c_3).$$

Here, the term

$$m(c_3) = \beta(c_3 \ln c_3 + \delta + \xi(x,t)) \tag{13}$$

accounts for DIS and determines the phase with smallest energy value. β, δ are positive constants and $m(c_3)$ is positive for small copper concentrations below a certain threshold x_1 and negative above it. Without stochastic source ξ this concept is due to Kobayashi [6] and the term $m(c_3)$ is discussed in our earlier article on chalcopyrite disease in sphalerite, see in particular Figure 3 therein. By adding the positive value $m(c_3)$ for a small copper concentration to f_1, chalcopyrite will less likely have the smallest free energy. Similarly, a negative value of $m(c_3)$ lowers the free energy and chalcopyrite is preferred.

In (13), the term $\xi(x,t)$ is the aforementioned small random fluctuation and can be regarded as the path of a Brownian motion.

4 Numerical simulations

In this section we present the results of a numerical simulation with high resolution that illustrates the characteristic properties of the model. The finite element triangulation of Ω as well as the time step Δt is not optimised during the computation run. The simulations are carried out for a two-dimensional layer Ω and (2)-(6) are solved in their dimensional form. For the physical parameters, the measured quantities were used.

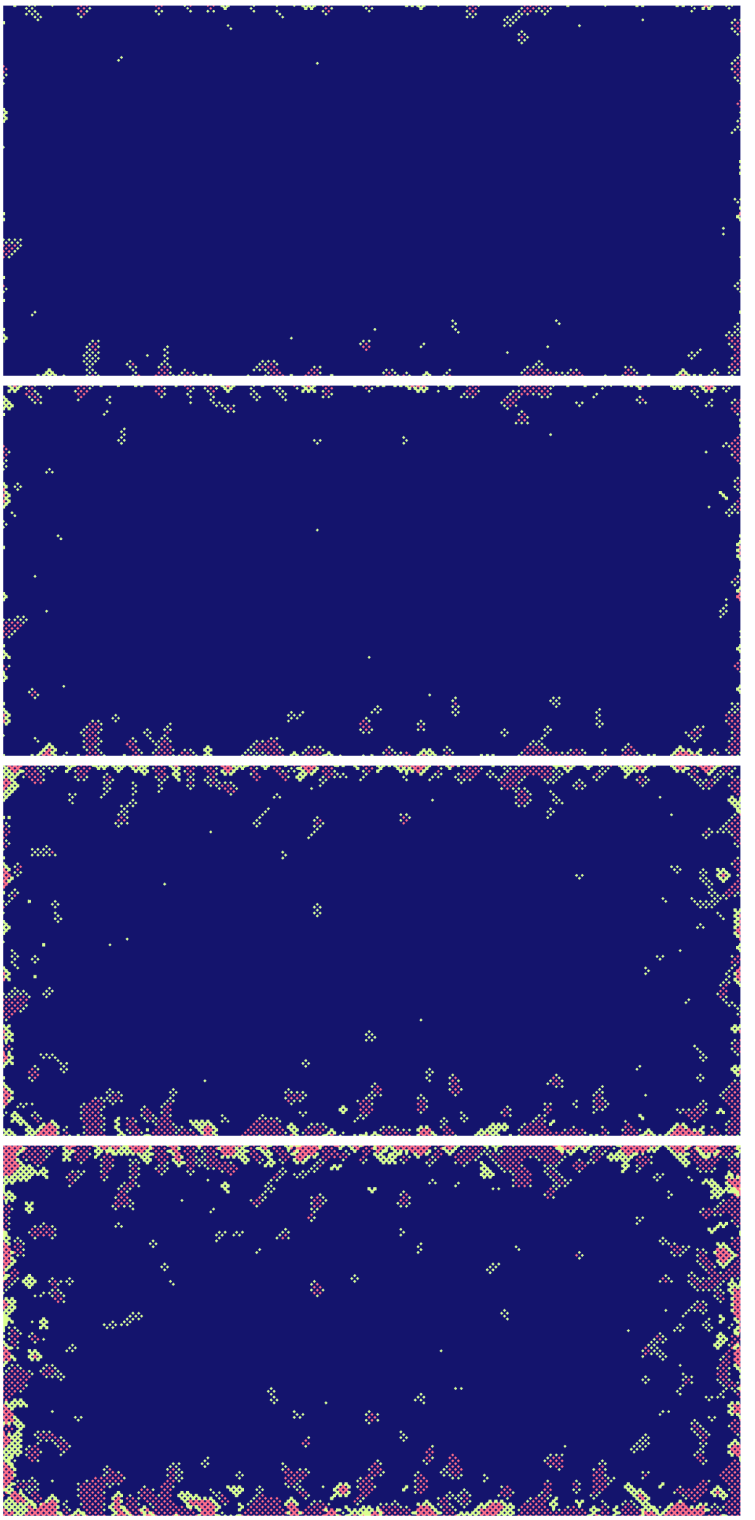

Fig. 7 Time evolution of the phase parameter from t=35d (top), t=60d, t=110d to t=190d (bottom). At t=0d only sphalerite(blue) is present (not displayed). As copper enters the crystal, chalcopyrite (red) forms close to the crystal boundary. Always a thin cubanite layer (green) is located in the interface between the other two phases. We can observe how the segregation starts with small islands that more and more concentrate until a connected front is formed.

The diffusivity constants were taken from the published data in [8]. The numerical implementation makes use of linear finite elements and a very efficient Quasi-Newton method that relies on GMRES to solve the linearized equations, see again [1] for details.

Physical Parameters: $\Omega = 1,2 \cdot 10^{-3} m \times 6 \cdot 10^{-4} m$, $T = 500°C$, $\varepsilon^2 = 3 \cdot 10^{-9} m$, $\alpha_3 = \alpha_4 = 0$,
$D_{CU} = 2.6 \cdot 10^{-4} m/s$, $D_{Zn} = 1.85 \cdot 10^{-7} m/s$, $D_{Fe} = 1.26 \cdot 10^{-4} m/s$, $\alpha_1 = 1$, $\alpha_2 = 0.9$.

Triangulation Data: 33153 points, 65536 triangles, $h = 10^{-8}$.

General Parameters: $\varepsilon_{GMRES} = 4 \cdot 10^{-5}$, $\Delta t = 4 \cdot 10^{-3}$, $\eta = 10^{-8}$, $\beta = 20$, $\delta = 4$.

Initial conditions: $c_{01} \equiv 0.001$, $c_{02} = 0.3$, $c_{03} = 0.001$ and χ_0 the global minimum of $\chi \mapsto F(c_0, \chi)$ according to Equation (3).

Boundary conditions: $\partial_n c_1 = \partial_n c_2 = 0$, $c_3 = 0.25$ and $\partial_n \chi_1 = \partial_n \chi_2 = 0$ on $\partial\Omega$.

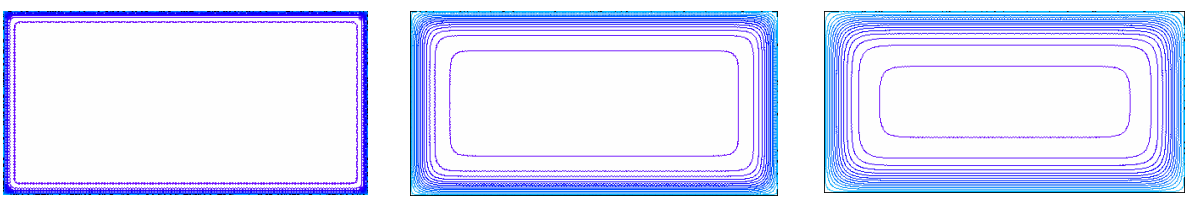

Fig. 8 Diffusion of Cu^+. The density of the level sets indicates the steepness of the copper gradient. At t=0d, the initial datum falls from 0.25 at the boundary to 0.001 in the centre.

The graph of Zn behaves opposite to the graph of Cu^+. It decreases near the boundary. The concentration of Fe^{3+} + Fe^{2+} is not displayed, it is a constant and invariant in time and space.

5 Discussion of the results and outlook

As presented above, the mathematical model is capable of capturing significant features of the ternary system in agreement with natural and experimental data. In experimental simulations of DIS-ccp, submicroscopic cubanite or corresponding phases may occur in status nascendi. As main result of our analysis, cubanite can be regarded as precursor to the formation of chalcopyrite. Those primary formed exsolutions are rapidly transformed by coarsening to visible DIS-phases as e.g. chalcopyrite or i.s.s. These results and interpretations agree with the presented mathematical simulations: The numerical implementation supplies a quantitative description of the physical process and gives fast predictions even in situations where the crystallographic experiments take very long. As result of the sharp interface model and the improved spatial resolution, the simulations can now even capture small islands of chalcopyrite that proceed the main front.

Nevertheless, the following aspects deserve a deeper investigation:

a) The model reflects DIS phenomena of sphalerite-cubanite-chalcopyrite on a medium spatial scale. The micro structure is not resolved and unknown from experiment.
b) The diffusivities of the constituents are assumed to be constant. As is well known, the actual physical parameters vary in space and depend on parameters on the micro scale. A correct representation in particular of the copper diffusion is a challenging task.
c) It is probable that the catalytic effect of cubanite on the decomposition of sphalerite and chalcopyrite has its root in the lattice geometry of the unit cell of these substances. This should be analysed by further experiments and ab initio computations.
d) The inhomogeneities are not purely random as assumed in our model. The precise knowledge about the coupling of $\xi(x,t)$ and other parameters (e.g. the Fe and Zn concentrations) would be of high importance

to improve the accuracy of the predictions by the model. Unfortunately, this objective seems to be extremely difficult to accomplish by in situ measurements. Yet there is hope that by careful mathematical investigations of the coupling between diffusion rates and size of the impurities for this ternary system, together with an application of the catalytic segregation principle derived in this article, more can be set about the early stages of segregation.

Acknowledgements This work is funded by the Deutsche Forschungsgemeinschaft under Lu 312/6-3 within the "Schwerpunktprogramm: Strukturgradienten".

References

[1] T. Blesgen, S. Luckhaus, and K. Bente, Cryst. Res. Technol. **37**, 570–580 (2002).
[2] K. Bente and T. Doering, Eur. J. Mineral. **10**, 465 (1993).
[3] K. Bente and T. Doering, Min. Petrol. **53**, 285–305 (1995).
[4] T. Blesgen, J. Phys. D **32**, 1119–1123 (1999).
[5] H. E. Cook, Acta Metall. **18**, 297–306 (1970).
[6] R. Kobayashi, Physica D, 410 (1993).
[7] J. S. Langer, Ann. Phys. **65**, 53–86 (1975).
[8] P. Nelkowski and S. Bollmann, Min. Petrol. 27 (1969).
[9] W. P. Ziemer, Weakly differentiable functions, Springer New York (1989).